

# Extraction of nanolignin from coconut fibers by controlled microbial hydrolysis



Siddhi J. Juikar, N. Vigneshwaran\*

Chemical and Biochemical Processing Division, ICAR-Central Institute for Research on Cotton Technology, Matunga, Mumbai 400019, India

## ARTICLE INFO

### Keywords:

*Aspergillus sp.*  
Coconut fibers  
Controlled microbial hydrolysis  
Homogenization  
Nanolignin  
Ultrasonication

## ABSTRACT

Biodegradable nanomaterials derived from biopolymers like cellulose, lignin, chitin and starch are hypothesized to support the development of eco-friendly functional nanosystem. In this work, nanolignin was extracted from coconut fibers by a controlled microbial hydrolysis process and compared with the nanolignins prepared by high shear homogenization and ultrasonication processes. The bulk lignin extracted from coconut fibers by soda pulping process was subjected to controlled hydrolysis by a lignin degrading fungal isolate, *Aspergillus sp.* The obtained nanolignin was characterized for size by DLS particle size analyzer, morphology by AFM and FE-SEM, chemical nature by FTIR, glass transition temperature by DSC and crystallite size by XRD. The microbial process yielded 58.4% nanolignin while homogenization and ultrasonication processes yielded 81.4% and 64.3%, respectively. Consequently, nanolignin, a value added compound can be extracted from coconut fibers to be used in textile, biomedical and environmental applications among others.

## 1. Introduction

While synthetic polymers have replaced the traditional metals and glass based materials for diversified applications due to low cost and ease of processing, increasing environmental concerns pave way for the emergence of biopolymers. There is a great potential of the biopolymer based nanomaterials to be used in nano-medicine due to their biocompatibility and biodegradability (Huang et al., 2015). Lignin is the most available biopolymer next only to cellulose and constitutes 25–30% of the non-fossil organic molecules on Earth. Its potential areas of applications include fillers in polymer composites, stabilizing agents, lubricants, coating additives, plasticizers and surfactants (Morandim-Giannetti et al., 2012; Thakur et al., 2014). While technologies are well established for conversion of carbohydrates to value-added products like pulp, sugar monomers and ethanol, lignin valorization process is less-developed and technical lignin are almost burnt for generation of heat and steam (Azadi et al., 2013). Currently, the pulp and paper industry liberates approximately 50 million tons of degraded lignin as part of the 130 million tons of kraft pulp produced annually (Brujninex et al., 2015).

Recently, nanolignin is gaining importance due to the ever-increasing demand for bio-based & bio-active nanomaterial fillers for use in bio-degradable composites. Though lignin in its native form is used as filler to increase the resistance of natural rubber vulcanizates to thermo-oxidative degradation in air (Košíková et al., 2007) and

functions like a chain extender and cross-linking agent for biopolyurethane molecules (Luo et al., 2013), nanolignin increased the thermal stability when blended with polyvinyl alcohol (PVA) more effectively, when compared to native lignin/PVA blends (Nair et al., 2014). Similarly, the incorporation of nanolignin in wheat gluten based bio-nanocomposites resulted in increased mechanical performance (tensile strength and modulus), improved thermal stability and reduced water sensitivity and present an excellent UV resistance (Yang et al., 2015). Also, nanolignin application for finishing process of linen fabrics helps to obtain multifunctional textile products having UV barrier, antibacterial, antistatic properties guaranteeing positive effect on human physiology (Zimniewska et al., 2008). Nanolignin infused with silver ions and coated with a cationic polyelectrolyte layer form a biodegradable and green alternative to silver nanoparticles. The polyelectrolyte layer promotes the adhesion of the particles to bacterial cell membranes and, together with silver ions, can kill a broad spectrum of bacteria, including *Escherichia coli*, *Pseudomonas aeruginosa* and quaternary-amine-resistant *Ralstonia sp* (Richter et al., 2015). Nanolignin preparation by acidic precipitation method was reported to result in biodegradable nanoparticles from lignin that are apparently non-toxic for microalgae and yeast (Frangville et al., 2012).

The recent methods explored for preparation of nanolignin include high shear homogenization (Nair et al., 2014), ultrasonic treatment (Zimniewska et al., 2008) and precipitation from an ethylene glycol solution by using dilute acidic aqueous solutions (Frangville et al.,

\* Corresponding author.

E-mail addresses: [Vigneshwaran.N@icar.gov.in](mailto:Vigneshwaran.N@icar.gov.in), [nvw75@yahoo.com](mailto:nvw75@yahoo.com) (N. Vigneshwaran).

2012). For application oriented synthesis, the lignin has been chemically modified by the esterification of its hydroxyl groups in order to both change the lignin solubility and increase the interaction with the polymer matrix in the nanocomposite (Nevárez et al., 2011). While the high shear homogenization and ultrasonic treatment protocols are energy intensive, chemical process releases toxic effluent in addition to modifying the surface chemistry of lignin. To the best of our knowledge, no reports appeared on the preparation of nanolignin by microbial process.

White-rot fungi are the most efficient degraders of lignin due to secretion of ligninolytic extracellular oxidizing enzymes. Two major groups of enzymes involved in lignin degradation are peroxidases and laccase (EC 1.10.3.2). Three peroxidases involved in lignin degradation are produced by white-rot fungi: Lignin peroxidase (LiP, EC 1.11.1.14), characterized by oxidation of high redox-potential aromatic compounds (including veratryl alcohol); manganese peroxidase (MnP, EC 1.11.1.13), that requires  $Mn^{2+}$  to complete the catalytic cycle and forms  $Mn^{3+}$  chelates acting as diffusing oxidizers; and, Versatile peroxidase (VP, EC 1.11.1.16) that oxidize  $Mn^{2+}$  as well as non-phenolic aromatic compounds, phenols and dyes (Martínez, 2002). MnP is the most common lignin-modifying peroxidase enzyme produced by almost all wood-colonizing basidiomycetes causing white-rot and various soil-colonizing litter-decomposing fungi (Hofrichter, 2002). But, very few research work reported the ability of *Aspergillus* sp. to synthesize hydrolytic enzymes of lignin (Zhang et al., 2015).

In this work, we have reported the preparation of nanolignin from coconut fibers by controlled microbial hydrolysis (fungal isolate: *Aspergillus* sp.) and their complete characterization. For comparison, nanolignin was prepared by two reported protocols, homogenization and ultrasonication.

## 2. Materials and methods

### 2.1. Lignin extraction

Extraction of lignin from coconut fiber was carried out by soda pulping process. Here, the coconut fibers were treated with sodium hydroxide at 170 °C followed by acid precipitation at pH 2.0. Lignin estimation was done as given in the standard TAPPI T-222 om-02. Thus extracted lignin is referred as 'bulk lignin' in further work.

### 2.2. Isolation of lignin degrading fungus

Compost samples prepared from cotton stalks (ICAR-Central Institute for Research on Cotton Technology, Mumbai, India) were used for isolation of lignin degrading microorganism. For enrichment, 2.5 g compost sample was added in 50 mL of sterile distilled water and kept in shaker for 1 min. The resulting suspension (0.5 mL) was added to 20 mL of modified mineral salts medium containing,  $NaNO_3$ , 1.5 g;  $MgSO_4 \cdot 7H_2O$ , 0.25 g;  $KH_2PO_4$ , 0.5 g;  $KCl$ , 0.25 g added with 0.01% (w/v) bulk lignin as sole carbon source and incubated at 27 °C for 7 days at 100 rpm (Henderson, 1961). The resulting fungal colonies were isolated and purified by single spore isolation method and sub cultured in Rose Bengal agar medium for further studies. Lactophenol cotton blue was used for fungal staining and based on the morphological observation, its characteristic conidiophore, the genus was identified to be *Aspergillus* sp.

### 2.3. Nanolignin extraction

Bulk lignin in aqueous suspension (7% concentration) was subjected to high shear homogenization at 10,000 rpm for 60 min in IKA T 25 digital ULTRA-TURRAX®. The resultant sample was allowed to settle for 1 h and only the supernatant was taken for analysis of nanolignin. For ultrasonication, the aqueous suspension of bulk lignin (7% concentration) was sonicated in an ultrasonic water bath (ELMA®, India) with

30 W power and 37 kHz frequency for 60 min. Subsequently, the sonicated sample was allowed to settle for 1 h and only the supernatant was taken for analysis of nanolignin. During both the homogenization and ultrasonication processes, the samples were kept in an ice bath to avoid the rise in temperature.

For microbial process, bulk lignin was used as the sole carbon source in basal medium (Tien and Kirk, 1988) for the fungal isolate *Aspergillus* sp., under shaking condition at 110 rpm for 31 °C for 15 days. The process was monitored on alternate days and the samples taken were analyzed. The samples were centrifuged at 1000 rpm for 15 min to remove biomass and un-hydrolyzed lignin. The supernatant was filtered through 1 µm filter and the filtrate containing nanolignin was taken for further analysis.

### 2.4. Lignin peroxidase (LiP) assay

The methylene blue reaction was used for analysis of LiP activity in the culture supernatant. For this purpose, the 2.7 mL of assay mixture contained 2.2 mL of supernatant, 0.1 mL of 1 mM methylene blue, 0.3 mL of 0.5 M sodium tartrate buffer (pH 4.0). The oxidative reaction was started by the addition of 0.1 mL of 4.5 mM  $H_2O_2$ . The colour that developed in the presence of LiP was compared to a blank assay, wherein double distilled water was used to replace the supernatant (Magalhães et al., 1996). Mixtures with LiP showed a change of colour from blue to greenish blue and then to purple blue.

### 2.5. Size and zeta potential analyses

The particle size distribution and zeta potential of nanolignin were measured using Nicomp™ 380 ZLS size analyzer by dynamic light scattering (DLS) principle. This instrument employs a design, which permits both multi-angle particle size analysis by DLS and low-angle zeta potential analysis by electrophoretic light scattering (ELS). Size calibration was carried out using 90 nm size polystyrene latex spheres and zeta potential calibration by using 491 nm polystyrene latex spheres. The size distribution was obtained based on the dynamic light scattering and autocorrelation principle. The mean diameter of the particles was calculated from their Brownian motion via the Stokes–Einstein equation. For this, HeNe laser (632.8 nm) was used and the scattering intensity was analysed by Avalanche photodiode detector at 90° orientation. To obtain the average size of bulk lignin, laser diffraction particle size analyzer (Microtrac S3500®) was used.

### 2.6. FTIR and XRD characterization

FTIR analysis was carried out in IRPrestige-21® in transmission mode using KBr pellets. Freeze dried nanolignin was pressed with KBr to form pellets and a total of 64 scans were taken per sample with a resolution of  $4\text{ cm}^{-1}$ . Wide angle X-ray diffraction patterns of nanolignin were obtained using a Philips® PW 1710 X-ray diffractometer with nickel filtered  $Cu\ K\alpha$  ( $\lambda = 1.54\text{ \AA}$ ) radiation and analyzed using automatic powder diffraction (APD) software. The diffracted intensities were recorded from 5° to 80° 2θ angles. The size of the crystallites in lignin can be calculated using the Scherrer formula given in Eq. (1).

$$\text{Mean size of crystallites} = \frac{k\lambda}{\beta \cos\theta} \quad (1)$$

Where, k is the shape factor and taken to be 0.9 for nanolignin,  $\lambda$  is the wavelength of X-ray (0.154 nm),  $\beta$  is the line broadening at half the maximum intensity (FWHM), after subtracting the instrumental line broadening, in radians and  $\theta$  is the Bragg angle (in degrees) (Goudarzi et al., 2014).

### 2.7. FEG-SEM, TEM and AFM analyses

Field Emission Gun – Scanning Electron Microscope (JEOL JSM-

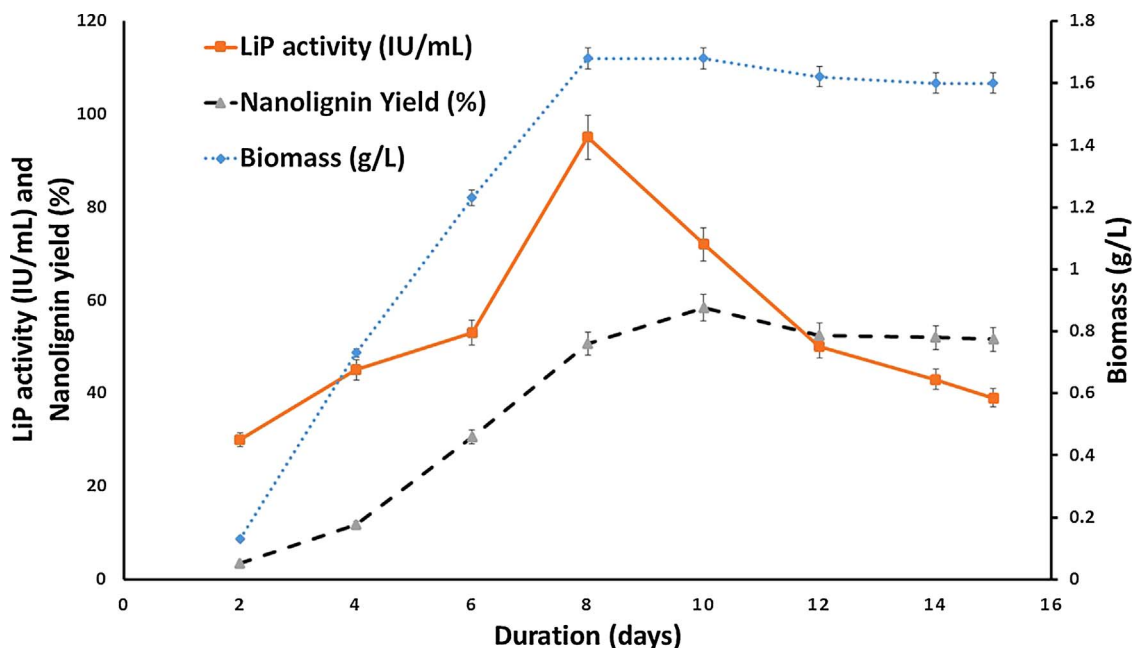


Fig. 1. LiP activity, nanolignin and biomass yield during nanolignin synthesis by controlled microbial hydrolysis.

7600F FEG-SEM) having a resolution of 1.0 nm at 15 kV was used to visualize the nanolignin morphology. The acceleration voltage was 10.0 kV. Transmission Electron Microscope (Philips CM 200<sup>®</sup>) was used to analyze the nanolignin after stained using uranyl acetate. AFM (Atomic force microscope) analysis was carried out in diInnova<sup>®</sup> SPM (Veeco, Santa Barbara, CA, US) equipped with a 90  $\mu$ m scanner by tapping mode in ambient condition. The silicon nitride cantilever with a spring constant of 40 Nm<sup>-1</sup> was used for scanning. The scan rate of 1.0 Hz and 512 lines per 5  $\mu$ m was used to optimum contrast. No filtering was done during scanning.

### 2.8. DSC analysis

Differential scanning calorimetry (DSC) of the samples was carried out using a DSC thermal analyzer (Mettler<sup>®</sup>). Approximately 5.0  $\pm$  0.2 mg samples were placed in a hermetic pan and sealed. DSC scans were performed at a heating rate of 10  $^{\circ}$ C/min from ambient to 300  $^{\circ}$ C under nitrogen atmosphere. The glass transition temperature of the samples were measured as onset temperatures of step change in heat capacity in the DSC trace.

## 3. Results and discussion

The emergence of bio-refinery projects to develop biofuels, bio-based materials and chemicals from carbohydrate polymers generates large amounts of lignin with a huge potential for value addition. These developments brought about renewed interest in the last decade for lignin and its potential use in polymer materials (Duval and Lawoko, 2014) and lignin-derived carbon materials, such as carbon fibers, carbon mats, activated carbons, carbon films, and templated carbon (Chatterjee and Saito, 2015). Value-added applications of lignin are also essential for the economic viability of future bio-refineries. It is however an under-utilized natural resource due to its structural heterogeneities (Zhao et al., 2016). Coconut fiber is a stiff coarse fiber found between the husk and the outer shell of a coconut. The inherent properties of these fibers include moth-proof, resistant to fungal attack, insulation & flame-retardant properties, tolerance to moisture and dampness. The raw coconut fibers contain 38% cellulose, 32% lignin, 25% hemicellulose, 0.5% pectin, 1.5% ash and the rest includes fats & waxes (Basu et al., 2015). The lignin extracted from coconut fibers finds

applications in adhesives, dispersants, and as additives in various chemical formulations.

In Nature, microorganisms have evolved mechanisms to both depolymerize lignin using extracellular oxidative enzymes and to uptake the aromatic species generated during depolymerization for carbon and energy sources (Salvachua et al., 2015). This work is focused on production of nanolignin out of bulk lignin by a microbiological way. The compost sample rich in ligninolytic microorganisms was enriched with bulk lignin and the resultant dominant fungal isolate was purified and characterized for their morphological attributes. Based on the conidial morphology, the genus of the purified isolate was identified as *Aspergillus* sp.

The fungal isolate was cultured in the medium containing lignin as sole carbon source and the enzyme activity (LiP) was monitored throughout the incubation period. LiP is an extracellular haem peroxidase and its activity can be monitored by cleavage or H<sub>2</sub>O<sub>2</sub>-dependent oxidation of a wide variety of model compounds. In the method followed, demethylation of methylene blue was used to quantitatively estimate the presence of LiP enzyme. This enzyme is responsible for degradation of lignin, which is essential for the size reduction to achieve nanolignin. The broth culture was sampled on alternative days and the broth was allowed to settle for an hour. After 1 h of sedimentation, the supernatant was removed to study the presence of nanolignin by analyzing its particle size, morphology, chemical structure and thermal properties. The yield was calculated on weight basis. For comparison, the high shear homogenization and ultrasonication processes were also used to produce nanolignin and characterized. The yields of nanolignin were 81.4%, 64.3% and 58.4% by high shear homogenization, ultrasonication and microbial processes, respectively. The comparatively low yield of nanolignin could be attributed to the fact that fungal isolate is consuming significant amount of bulk lignin for its growth and converted into biomass. This is in similar line with our earlier finding on the production of nanocellulose from microcrystalline cellulose by controlled microbial hydrolysis (Satyamurthy et al., 2011).

Fig. 1 shows the LiP activity, nanolignin and biomass yield during nanolignin synthesis by controlled microbial hydrolysis. The LiP activity was at its peak on eighth day of incubation after which, it got reduced. Similarly the biomass yield also achieved its peak on day 8 and then, it progressed in a steady-state. The yield of nanolignin increased

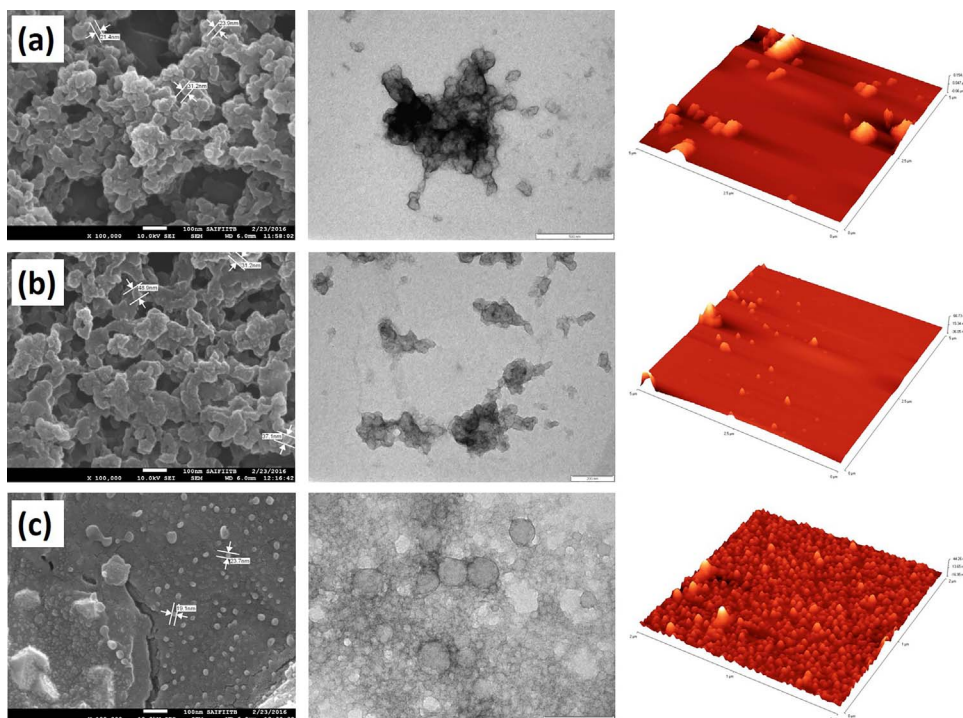


**Fig. 2.** FEG-SEM (first column), TEM (second column) and AFM (last column) micrographs of nanolignins prepared by homogenization (a), ultrasonication (b) and microbial (c) processes. Scale bars of FEG-SEM micrographs correspond to 100 nm; TEM micrographs correspond to 200 nm (except for 'a', where it is 500 nm); and, AFM micrographs corresponds to  $5\ \mu\text{m} \times 5\ \mu\text{m}$  in x-y directions.

till 10 days of incubation and later, it maintained a steady-state with slight reduction in quantity. The overall nanolignin yield was low when compared to other two methods of preparation because of the fact that the fungus utilized lignin for its growth purpose and converted into fungal biomass.

The representative micrographs of nanolignins observed by FEG-SEM, TEM and AFM are given in Fig. 2. FEG-SEM micrographs of nanolignins prepared by homogenization and ultrasonication showed aggregation of particles while that of microbial process showed well dispersed particles. This result was supported by TEM and AFM analyses. The average sizes of nanolignins are given in Table 1. The contrast for nanolignins in TEM was obtained using the addition of uranyl acetate. For comparison, the average sizes obtained by DLS technique is also given in Table 1. The nanolignins prepared by homogenization and ultrasonication showed three peaks indicating the probable aggregation of particles while only two peaks appeared in that of microbial process. Also, the sizes obtained in peak #1 of DLS technique were comparable to that of microscopic analyses. First column in Fig. 3 shows the average size graphs obtained using DLS analysis for the nanolignin produced by three different processes and that of bulk lignin analyzed by laser diffraction method. The size of the bulk lignin was in the range of 2–150  $\mu\text{m}$  having the peak around 55  $\mu\text{m}$ .

FTIR analysis was carried out to understand the chemical characteristics of both bulk lignin and nanolignin prepared by three different processes. The lignin exhibits prominent bands at  $3000\text{--}3600\ \text{cm}^{-1}$  (the stretching vibrations of the hydroxyl group),  $1700\ \text{cm}^{-1}$  (C=O stretching)  $1598\ \text{cm}^{-1}$  (aromatic skeletal vibration),  $1514\ \text{cm}^{-1}$  (C–C stretching of aromatic skeletal),  $1460\ \text{cm}^{-1}$  (C–H

stretching of aromatic skeletal), and  $1425\ \text{cm}^{-1}$  (aromatic skeletal vibrations combined with C–H in-plane deformation) (Zhou et al., 2015). As per the FTIR spectra given in Fig. 3, it was observed that the intensity of the peak in  $3000\text{--}3600\ \text{cm}^{-1}$  due to stretching vibrations of the hydroxyl group has increased in all nanolignins due to the more amount of moisture being held by the nanolignins. Other peaks suggested that the chemical nature of both bulk lignin and the synthesized nanolignins was identical.

The XRD analyses of bulk lignin and nanolignins are given in Fig. 3 and Table 2. The bulk lignin has very broad hump corresponding to that of amorphous region present in its structure. All nanolignins showed prominent peaks around region  $22.5\text{--}23.0$  ( $2\theta$ ) due to increased amount of crystalline regions in their structures. This peak corresponds to the stacking structure of aromatic layers (Hu et al., 2014). The process of nanolignin preparation involved the destruction of primary structure by homogenization, ultrasonication or hydrolysis that primarily removed the amorphous regions. Also, the plasticization of lignin due to moisture and re-drying helped in increasing the orderliness and hence, the increased crystalline region in nanolignins. The size of the crystallites is lowest in case of ultrasonication (1.50 nm) and highest in case of microbial process (3.92 nm). The very high disruptive energy provided by ultrasonication process might have disturbed the crystalline region existed in the bulk lignin, hence, the smallest size. The obtained results (sizes of the crystallites of lignin samples obtained from coconut fibers) are comparatively high when compared to that of kraft lignin samples obtained from softwood (0.71 nm) and hardwood (0.75 nm) as reported earlier (Goudarzi et al., 2014).

Lignin is an amorphous polymer and undergoes changes on heating,

**Table 1**  
Size analyses of nanolignins by microscopy and DLS technique.

Nanolignin preparation methods	Average particle size (nm) by image analysis			Size (nm) by DLS analysis		
	FEG-SEM	TEM	AFM	Peak #1	Peak #2	Peak #3
Homogenization	$26.5 \pm 7.5$	$31.8 \pm 11.2$	$88.5 \pm 31.2$	$25.3 \pm 2.0$	$259.4 \pm 22.1$	$1858.0 \pm 120.0$
Ultrasonication	$35.8 \pm 7.8$	$58.6 \pm 13.5$	$45.8 \pm 29.9$	$44.7 \pm 3.2$	$643.9 \pm 77.8$	$1849.2 \pm 85.8$
Controlled microbial hydrolysis	$22.3 \pm 6.5$	$25.8 \pm 8.9$	$28.0 \pm 8.3$	$27.5 \pm 2.7$	$207.4 \pm 17.1$	No peak

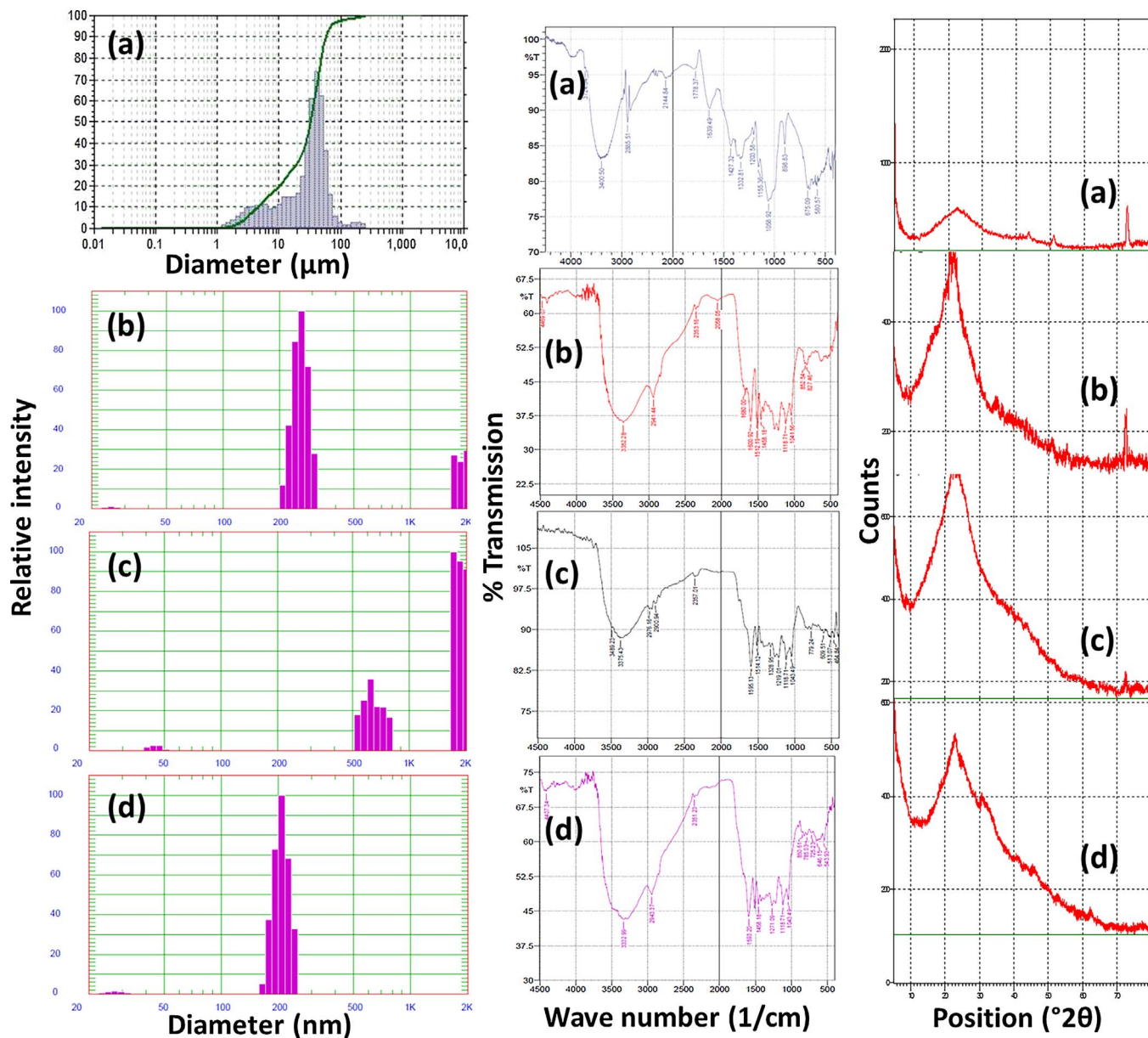


Fig. 3. Particle size (first column), FTIR (second column) and XRD (last column) spectra of bulk lignin (a) and nanolignins prepared by homogenization (b), ultrasonication (c) and microbial (d) processes.

Table 2  
XRD analysis of nanolignins.

Process of synthesis of nanolignins	Position of the peak (°2θ)	d-spacing (Å)	Size of crystallites (nm)
Bulk lignin	22.5	3.89	3.01
Homogenization	22.5	3.96	3.70
Ultrasonication	22.9	3.88	1.50
Microbial hydrolysis	22.8	3.89	3.92

resulting in transition to a glassy and rubbery state. Tg is defined as the onset of major change in heat capacity in DSC traces. The glass transition temperature (Tg) appears around 147–172 °C for coconut husk lignin depending on extraction process and presence of low molecular weight contaminants (Vázquez-Torres et al., 1992). In our work (Fig. 4), the Tg of bulk lignin was 139.7 °C and it increased to 156.6 °C, 156.5 °C and 156.2 °C for the nanolignins prepared by homogenization, ultrasonication and controlled microbial hydrolysis, respectively. The

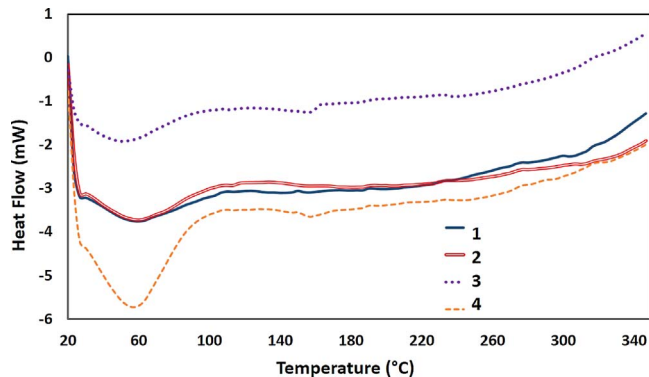


Fig. 4. DSC thermograms of bulk lignin (1), nanolignin by homogenization (2), nanolignin by ultrasonication (3), and nanolignin by controlled microbial hydrolysis (4).

increase in glass transition temperature on size reduction is in agreement with the earlier findings where the T<sub>g</sub> of kraft lignin (120 °C) increased to 154 °C after subjected to mechanical shearing by high shear homogenization for production of nanolignin (Nair et al., 2014). No significant difference among the T<sub>g</sub> of nanolignins concludes that the three different processes does not affect the glass transition temperature of the final product, nanolignin.

#### 4. Conclusions

Rational design of the functionalized lignin-based materials will lead to a rich family of hybrid functional carbon materials with various applications toward a green and sustainable future (Liu et al., 2015). Lignin is being explored for diversified applications such as controlled release, saccharification of lignocelluloses, bioplastics, composites, nanoparticles, adsorbents and dispersants, in electro-chemical applications and carbon fibers (Norgren and Edlund, 2014). Nanolignin adds a new dimension to the use of biomass as a value-added product having diversified areas of applications ranging from composites to medical applications. This work reported a newer means of synthesis of nanolignin from bulk lignin extracted from coconut fibers, by controlled microbial hydrolysis. The reported microbial process is energy-efficient and environment friendly way of preparing nanolignin and this process is amenable for extending to lignins derived from various other sources like wood and agro-biomass.

Therefore, extraction of nanolignin from coconut fibers by a controlled microbial hydrolysis process proves to be an eco-friendly protocol having potential applications not only in conventional industries but also for textile, biomedical and environmental applications.

#### Acknowledgements

Authors thank Dr. P.G. Patil, Director and Dr. Sujata Saxena, Principal Scientist of ICAR-Central Institute for Research on Cotton Technology for their support and guidance during the research work. Authors also thank Mr. A. Arputharaj, Dr. N.M. Ashtaputre, Dr. Charlene D' Souza, Mr. Manoj Ambare, Mrs. Sujata Kawlekar and Mr. Nishant Kambli for their technical support to carry out the research work.

#### References

Azadi, P., Inderwildi, O.R., Farnood, R., King, D.A., 2013. Liquid fuels, hydrogen and chemicals from lignin: a critical review. *Renew. Sustain. Energy Rev.* 21, 506–523.  
 Basu, G., Mishra, L., Jose, S., Samanta, A.K., 2015. Accelerated retting cum softening of coconut fibre. *Ind. Crops Prod.* 77, 66–73.  
 Bruijninx, P.C.A., Rinaldi, R., Weckhuysen, B.M., 2015. Unlocking the potential of a sleeping giant: lignins as sustainable raw materials for renewable fuels, chemicals and materials. *Green Chem.* 17, 4860–4861.  
 Chatterjee, S., Saito, T., 2015. Lignin-derived advanced carbon materials. *Chem. Sus. Chem.* 8, 3941–3958.  
 Duval, A., Lawoko, M., 2014. A review on lignin-based polymeric, micro- and nano-structured materials. *React. Funct. Polym.* 85, 78–96.  
 Frangville, C., Rutkevičius, M., Richter, A.P., Velev, O.D., Stoyanov, S.D., Paunov, V.N., 2012. Fabrication of environmentally biodegradable lignin nanoparticles. *Chem. Phys. Chem.* 13, 4235–4243.

Goudarzi, A., Lin, L.-T., Ko, F.K., 2014. X-Ray diffraction analysis of kraft lignins and lignin-derived carbon nanofibers. *J. Nanotechnol. Eng. Med.* 5 021006-021006-021005.  
 Henderson, M.E.K., 1961. Isolation, identification and growth of some soil hyphomycetes and yeast-like fungi which utilize aromatic compounds related to lignin. *Microbiology* 26, 149–154.  
 Hofrichter, M., 2002. Review: lignin conversion by manganese peroxidase (MnP). *Enzyme Microb. Technol.* 30, 454–466.  
 Hu, J., Shen, D., Wu, S., Zhang, H., Xiao, R., 2014. Effect of temperature on structure evolution in char from hydrothermal degradation of lignin. *J. Anal. Appl. Pyrolysis* 106, 118–124.  
 Huang, Y., Wang, Y.-J., Wang, Y., Yi, S., Fan, Z., Sun, L., Lin, D., Anreddy, N., Zhu, H., Schmidt, M., Chen, Z.-S., Zhang, M., 2015. Exploring naturally occurring ivy nanoparticles as an alternative biomaterial. *Acta Biomater.* 25, 268–283.  
 Košíková, B., Gregorová, A., Osvald, A., Krajčovičová, J., 2007. Role of lignin filler in stabilization of natural rubber?based composites. *J. Appl. Polym. Sci.* 103, 1226–1231.  
 Liu, W.-J., Jiang, H., Yu, H.-Q., 2015. Thermochemical conversion of lignin to functional materials: a review and future directions. *Green Chem.* 17, 4888–4907.  
 Luo, X., Mohanty, A., Misra, M., 2013. Lignin as a reactive reinforcing filler for water-blown rigid biofoam composites from soy oil-based polyurethane. *Ind. Crops Prod.* 47, 13–19.  
 Magalhães, D.B., de Carvalho, M.E.A., Bon, E., Neto, J.S.A., Kling, S.H., 1996. Colorimetric assay for lignin peroxidase activity determination using methylene blue as substrate. *Biotechnol. Tech.* 10, 273–276.  
 Martínez, A.T., 2002. Molecular biology and structure-function of lignin-degrading heme peroxidases. *Enzyme Microb. Technol.* 30, 425–444.  
 Morandim-Giannetti, A.A., Agnelli, J.A.M., Lanças, B.Z., Magnabosco, R., Casarin, S.A., Bettini, S.H.P., 2012. Lignin as additive in polypropylene/coir composites thermal, mechanical and morphological properties. *Carbohydr. Polym.* 87, 2563–2568.  
 Nair, S.S., Sharma, S., Pu, Y., Sun, Q., Pan, S., Zhu, J.Y., Deng, Y., Ragauskas, A.J., 2014. High shear homogenization of lignin to nanolignin and thermal stability of nanolignin-polyvinyl alcohol blends. *Chem. Sus. Chem.* 7, 3513–3520.  
 Nevárez, L.A.M., Casarrubias, L.B., Celzard, A., Fierro, V., Muñoz, V.T., Davila, A.C., Lubian, J.R.T., Sánchez, G.G., 2011. Biopolymer-based nanocomposites: effect of lignin acetylation in cellulose triacetate films. *Sci. Technol. Adv. Mater.* 12, 045006.  
 Norgren, M., Edlund, H., 2014. Lignin: recent advances and emerging applications. *Curr. Opin. Colloid Interface Sci.* 19, 409–416.  
 Richter, A.P., Brown, J.S., Bharti, B., Wang, A., Gangwal, S., Houck, K., Cohen Hubal, E.A., Paunov, V.N., Stoyanov, S.D., Velev, O.D., 2015. An environmentally benign antimicrobial nanoparticle based on a silver-infused lignin core. *Nat. Nano* 10, 817–823.  
 Salvachua, D., Karp, E.M., Nimlos, C.T., Vardon, D.R., Beckham, G.T., 2015. Towards lignin consolidated bioprocessing: simultaneous lignin depolymerization and product generation by bacteria. *Green Chem.* 17, 4951–4967.  
 Satyamurthy, P., Jain, P., Balasubramanya, R.H., Vigneshwaran, N., 2011. Preparation and characterization of cellulose nanowhiskers from cotton fibres by controlled microbial hydrolysis. *Carbohydr. Polym.* 83, 122–129.  
 Thakur, V.K., Thakur, M.K., Raghavan, P., Kessler, M.R., 2014. Progress in green polymer composites from lignin for multifunctional applications: a review. *ACS Sustain. Chem. Eng.* 2, 1072–1092.  
 Tien, M., Kirk, T.K., 1988. Lignin peroxidase of *Phanerochaete chrysosporium*. *Methods Enzymol.* 161, 238–249.  
 Vázquez-Torres, H., Canché-Escamilla, G., Cruz-Ramos, C.A., 1992. Coconut husk lignin. I. Extraction and characterization. *J. Appl. Polym. Sci.* 45, 633–644.  
 Yang, W., Kenny, J.M., Puglia, D., 2015. Structure and properties of biodegradable wheat gluten bionanocomposites containing lignin nanoparticles. *Ind. Crops Prod.* 74, 348–356.  
 Zhang, Z., Xia, L., Wang, F., Lv, P., Zhu, M., Li, J., Chen, K., 2015. Lignin degradation in corn stalk by combined method of H<sub>2</sub>O<sub>2</sub> hydrolysis and *Aspergillus oryzae* CGMCC5992 liquid-state fermentation. *Biotechnol. Biofuels* 8, 183.  
 Zhao, W., Simmons, B., Singh, S., Ragauskas, A., Cheng, G., 2016. From lignin association to nano-/micro-particle preparation: extracting higher value of lignin. *Green Chem.* 18, 5693–5700.  
 Zhou, C., Jiang, W., Via, B.K., Fasina, O., Han, G., 2015. Prediction of mixed hardwood lignin and carbohydrate content using ATR-FTIR and FT-NIR. *Carbohydr. Polym.* 121, 336–341.  
 Zimmiewska, M., Kozłowski, R., Batog, J., 2008. Nanolignin modified linen fabric as a multifunctional product. *Mol. Cryst. Liq. Cryst.* 484, 43/[409]–450/[416].